


Development and Application of a Life-Stage Physiologically Based Pharmacokinetic (PBPK) Model to the Assessment of Internal Dose of Pyrethroids in Humans

Pankajini Mallick,^{*,1} Marjory Moreau,^{*,1,2} Gina Song,^{*,†} Alina Y. Efremenko,^{*} Salil N. Pendse,^{*} Moire R. Creek,[‡] Thomas G. Osimitz,[§] Ronald N. Hines ,[¶] Paul Hinderliter,^{||} Harvey J. Clewell,^{|||} Brian G. Lake,^{|||} and Miyoung Yoon^{*,†}

^{*}ScitoVation, LLC, Research Triangle Park, North Carolina 27709; [†]ToxStrategies, Cary, North Carolina 27511; [‡]Moire Creek Toxicology Consulting Services, Lincoln, California 95648; [§]Science Strategies, LLC, Charlottesville, Virginia 22902; [¶]US EPA, ORD, NHEERL, Research Triangle Park, North Carolina 27709; ^{||}Syngenta, Greensboro, North Carolina 27409; ^{|||}Ramboll, Research Triangle Park, North Carolina 27709; and ^{|||}Faculty of Health and Medical Sciences, University of Surrey, Surrey, UK

¹These authors contributed equally to this study as cofirst authors.

²To whom correspondence should be addressed at Pharmacology, Metabolism & Pharmacokinetics Division, 100 Capitola Drive Suite 106, Durham, NC 27713. Tel: 919-354-5220. E-mail: mmoreau@scitovation.com.

ABSTRACT

To address concerns around age-related sensitivity to pyrethroids, a life-stage physiologically based pharmacokinetic (PBPK) model, supported by *in vitro* to *in vivo* extrapolation (IVIVE) was developed. The model was used to predict age-dependent changes in target tissue exposure of 8 pyrethroids; deltamethrin (DLM), *cis*-permethrin (CPM), *trans*-permethrin, esfenvalerate, cyphenothrin, cyhalothrin, cyfluthrin, and bifenthrin. A single model structure was used based on previous work in the rat. Intrinsic clearance (CL_{int}) of each individual cytochrome P450 or carboxylesterase (CES) enzyme that are active for a given pyrethroid were measured *in vitro*, then biologically scaled to obtain *in vivo* age-specific total hepatic CL_{int} . These IVIVE results indicate that, except for bifenthrin, CES enzymes are largely responsible for human hepatic metabolism (>50% contribution). Given the high efficiency and rapid maturation of CESs, clearance of the pyrethroids is very efficient across ages, leading to a blood flow-limited metabolism. Together with age-specific physiological parameters, in particular liver blood flow, the efficient metabolic clearance of pyrethroids across ages results in comparable to or even lower internal exposure in the target tissue (brain) in children than that in adults in response to the same level of exposure to a given pyrethroid (C_{max} ratio in brain between 1- and 25-year old = 0.69, 0.93, and 0.94 for DLM, bifenthrin, and CPM, respectively). Our study demonstrated that a life-stage PBPK modeling approach, coupled with IVIVE, provides a robust framework for evaluating age-related differences in pharmacokinetics and internal target tissue exposure in humans for the pyrethroid class of chemicals.

Key words: PBPK modeling; pyrethroids; enzyme ontogeny; IVIVE.

Physiologically based pharmacokinetic (PBPK) modeling offers a framework to integrate mechanistic data for physiology and biochemical processes and serves as a tool to predict internal exposure at target tissues for a wide range of exposure conditions in animals or humans (Clewell and Andersen, 1994). In particular, PBPK models are an effective way to evaluate the potential impact of age-specific pharmacokinetics on internal exposure and to support risk assessment for potentially sensitive populations, such as younger ages (Hines et al., 2010; Yoon and Clewell, 2016). Modeling-based approaches address some of the challenges associated with using juvenile animal studies to infer the sensitivity in human children, such as species differences in maturation of physiology and biochemistry. *In vitro* to *in vivo* extrapolation (IVIVE) and *in silico*-based parameterization allows efficient development of PBPK models (Houston and Galetin, 2008; Yoon et al., 2012), especially for children where *in vivo* data generation is not possible (Ring et al., 2017; Yoon and Clewell, 2016).

Pyrethroids are among the most commonly used insecticides (Ratelle et al., 2015a,b). They act on the nervous system principally by interacting with voltage-gated sodium channels (Soderlund, 2012). High dose studies have shown increased lethality in juvenile rats, raising the possibility of potential age sensitivity. Lethality was observed in 11- and 21-day old rats (LD50 of 5.1 and 11 mg/kg, respectively) at significantly lower doses than in adult rats (LD50 of 81 mg/kg) (Sheets et al., 1994). It is thus important to characterize the basis for this greater sensitivity in younger rats and assess its relevance to humans. Such observations could be the result of age-related pharmacokinetic differences as it is known that species differences exists in pyrethroids metabolism and its ontogeny (Crow et al., 2007; Godin et al., 2006; Hines, 2013; Saghir et al., 2012). Our approach (Figure 1) combining life-stage PBPK modeling and IVIVE allows the incorporation of human relevant metabolism data and age-dependent physiological changes, thereby improving predictability of age-specific target tissue exposure. Species differences in the enzymes involved in pyrethroid metabolism (Crow et al., 2007; Godin et al., 2006) and the differential enzyme ontogeny reported between rats and humans suggest that metabolic competency in humans develops much earlier after birth compared with rats (Hines, 2013; Pope et al., 2005; Saghir et al., 2012; Yang et al., 2009). This illustrates a critical limitation in using neonatal animal toxicity studies to infer human early-life sensitivity. Life-stage IVIVE-PBPK modeling thus provides an improved platform as it appropriately incorporates species and age-specific profiles when evaluating age-specific internal exposure to support risk assessment of pyrethroids in early ages.

Instead of developing a compound-specific PBPK model for each pyrethroid, we applied a single model structure to 8 pyrethroids (deltamethrin [DLM], cis-permethrin [CPM], bifenthrin, trans-permethrin [TPM], esfenvalerate, λ -cyhalothrin, β -cyfluthrin, and cyphenothrin) along with both compound-independent and compound-specific parameters. This single model structure is found in the graphical representation of our approach (Figure 1) as the generic life-stage PBPK model for pyrethroids. This approach was also previously demonstrated in the rat (Song et al., 2019).

MATERIALS AND METHODS

Structure of the Life-Stage PBPK Model

The structure of the human life-stage PBPK model for pyrethroids is shown in Figure 2. This multicompartmental model

describes compound absorption and disposition in the body and incorporates a large data set of anatomical and physiological parameters with their age dependencies. The current model can simulate pyrethroid kinetics through oral ingestion and inhalation in single or multiple daily exposure scenarios and incorporates age-dependent human physiology, as well as maturation profiles of pyrethroid metabolism mediated by carboxylesterase (CES) and cytochrome P450 (CYP) enzymes in liver. Key assumptions of this human model structure and parameters are based on those evaluated in the rat model (Song et al., 2019). The model includes plasma and six tissue compartments: gastrointestinal tract, liver, fat, brain, slowly and rapidly perfused tissues. This multicompartmental model accounts for organ plasma flow rates and permeation into the organ tissue across a membrane between interstitial and cellular volume to achieve the right partitioning kinetics.

One salient feature of the model is inclusion of lymphatic absorption. Pyrethroids are highly lipophilic, therefore a certain fraction of the dose would be considered to be absorbed through the lymphatic pathway directly into the plasma compartment, by-passing the hepatic first pass metabolism (Charman and Stella, 1986; Jandacek et al., 2009; O'Driscoll, 2002). The lymphatic absorption contribution via ingestion is assumed to be 100% in rats (Song et al., 2019). The rat assumption is based on oral gavage dosing, where the exposure occurs with a bolus lipid intake (corn oil) and generally at higher doses. This assumption is unrealistic for humans, where oral exposure occurs with a wide variety of lipid intake. In humans, the degree of lymphatic absorption would be more similar to lipid emulsion-based exposure rather than oil gavage with a substantial variability expected. The fraction of lymphatic absorption in humans was derived based on literature data (O'Driscoll, 2002) with a mean around 10%. O'Driscoll (2002) showed that the degree of intestinal lymphatic transport of highly lipophilic drugs and chemicals on coadministration of lipid-based formulations or in presence of food ranges from 1% to 45% suggesting a substantial degree of human variability in the degree of lymphatic absorption.

Based on the rat modeling "restrictive clearance" of a pyrethroid was included in the model structure. Initial evaluation of the IVIVE in rats showed that *in vivo* metabolic clearance of DLM, CPM, and TPM was lower than anticipated from *in vitro* estimated metabolic clearance. In other words, clearance of these pyrethroids appears to be restricted by one or more factors *in vivo* not accounted for in the initial model (Song et al., 2019). Three important parameters used to define the restrictive clearance of a pyrethroid are (1) an empirical adjustment factor (KMF) that reduces free concentration for metabolism in the liver, (2) the free fraction of the compound in plasma that is available for tissue uptake (FuPLS), and (3) as explained above, a by-pass of hepatic first pass effect due to lymphatic absorption. In contrast to the KMF and lymphatic absorption values, which were estimated based on rat *in vivo* data and *in vitro* metabolism data, the FuPLS value is from human studies (Sethi et al., 2016). Full details of the study can be found elsewhere (Sethi et al., 2016), which states that the fraction unbound in plasma (FuPLS) was significantly higher (2–2.5X) at birth to 1 week but reached and remained at adult levels in infants and children older than 4 weeks of age. Because the youngest age group included in the PBPK model is 6-month-old infants, the age-dependent effects of plasma protein binding are not relevant to our simulation. Therefore, we used a FuPLS of 0.1 in all the simulated ages in this study. Because KMF is an adjustment of enzyme affinity for the free concentration reflecting the difference between *in vitro* and *in vivo* conditions, a similar assumption of age-

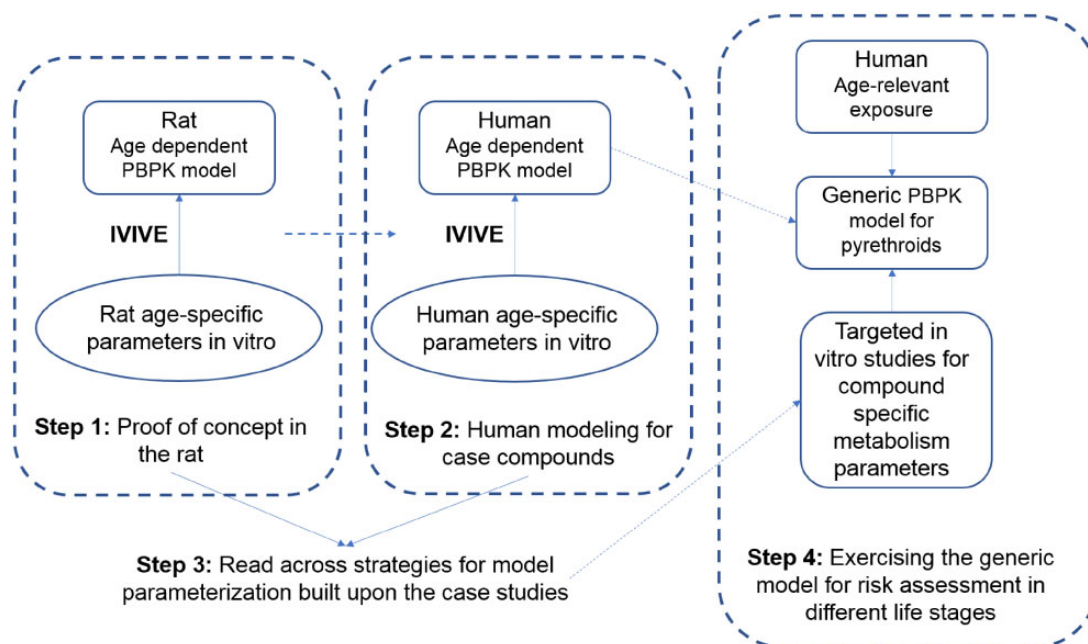


Figure 1. The approach building a generic physiologically based pharmacokinetic (PBPK) model for pyrethroids.

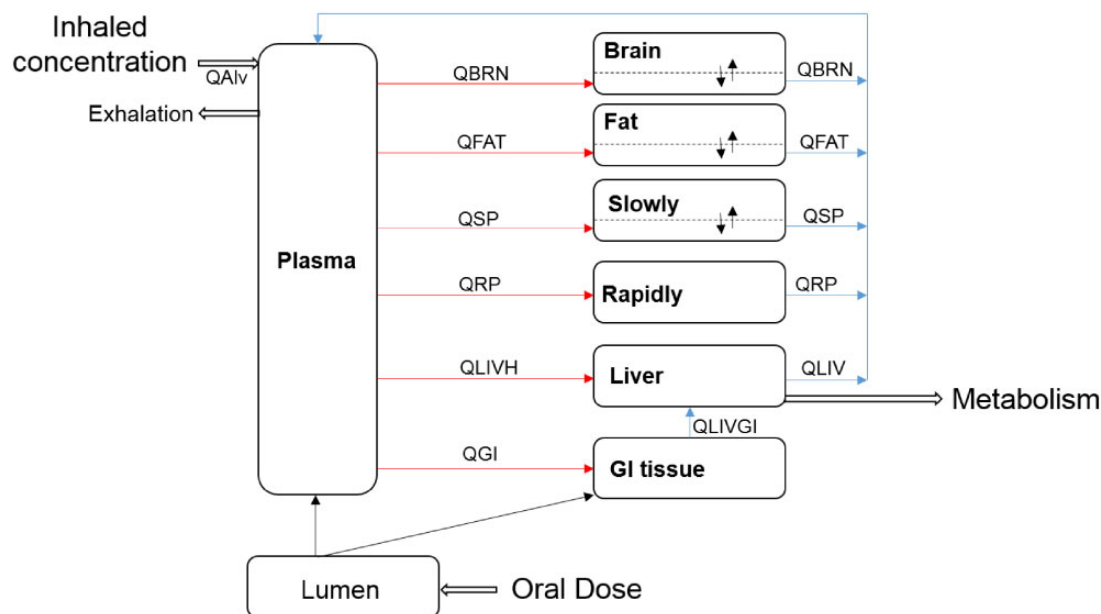


Figure 2. Structure of the generic life-stage PBPK model for pyrethroids in humans. QLIVGI, QLIVH, QRP, QSP, QFAT, and QBRN refer to plasma flow to each tissue compartment. QLIV is the sum of QLIVGI and QLIVH. QAlv refers to the alveolar ventilation rate. Brain, fat, and slowly perfused tissue compartments are described as diffusion-limited tissues (the dotted lines represent the separation between tissue [intracellular space] and blood tissue [extracellular space]), whereas all other tissue compartments are described as flow limited.

independence was appropriate. The fractional binding is not changing with age after 4 weeks and the unadjusted enzyme affinity is dependent on the shape and other characteristics of the active site, which is genetically controlled and does not vary with age. With respect to lymphatic absorption, the degree of intestinal lymphatic absorption can be influenced by digestibility of lipid-based vehicle as shown in rat studies because lipid content/type in the gut lumen affects the degree of stimulation of chylomicron production in enterocytes (Charman and Stella, 1986; Jandacek et al., 2009). Therefore, we can assume that the

principal factor affecting lymphatic absorption is the lipid content of the food, not age. Once weaned, the lipid content of the food in the gut would not be different between children and adults.

The PBPK model describes only the plasma compartment, unlike the previously published Tornero-Velez et al. (2012) that described the plasma and red blood cell (RBC) lumped into a whole-blood compartment. The RBC compartment was not included, as the data available in Mirfazaelian et al. (2006) do not support substantial concentrations of DLM in RBCs, hence,

elimination of the RBC compartment would not have much impact on the model predictions. Concentration of chemical in the plasma, RBCs, and whole blood can be defined using equation: $C_{\text{blood}} = C_{\text{plasma}} \times (1 - \text{HCT}) + C_{\text{RBC}} \times \text{HCT}$; where C describes concentrations (μM) and HCT (hematocrit). In cases where 100% of pyrethroids partition to the RBCs $C_{\text{plasma}} = 0$, $C_{\text{blood}} = 0.45 \times C_{\text{RBC}}$, and $C_{\text{plasma}}/C_{\text{blood}} = 0$. Whereas, if 100% partition to the plasma is assumed, $C_{\text{RBC}} = 0$ and $C_{\text{blood}} = 0.55 \times C_{\text{plasma}}$, and $C_{\text{plasma}}/C_{\text{blood}} = 1.82$. Thus, if there is no partitioning of DLM to RBCs, the ratio of plasma to blood concentration should be approximately 1.8 in Mirfazaelian *et al.* study. However, the actual ratio from the data extrapolated from the paper is 2.1. The lack of exact concordance between these numbers can be attributed to variability in measurement and/or hematocrit. Hence, the available data do not support substantial concentrations in RBCs and are more consistent with DLM being almost exclusively confined to plasma. Based on this analysis of the *in vivo* results from Mirfazaelian *et al.* (2006), we can conclude that the elimination of the RBC compartment has minimal impact on the model predictions. Furthermore, a nonpublished study has characterized the partitioning of DLM and CPM between erythrocytes and plasma *in vitro* and shows that DLM and CPM distributed evenly between RBC and plasma. The partition coefficient plasma:RBC was around 1.1 for DLM and between 0.5 and 1.1 for CPM. Willemin *et al.* (2016) also shows a PBPK model of pyrethroid lumping RBC and plasma into blood.

Distribution in the flow-limited model is through plasma flow mainly, whereas the diffusion-limited model includes an additional term to describe diffusion through a capillary membrane. In our model, brain, fat, and slowly perfused compartments are described as diffusion limited to appropriately describe the time-delay in equilibration of pyrethroid concentrations between these tissues and plasma that is observed in the rat (Kim *et al.*, 2008, 2010).

Elimination of pyrethroids occurs through metabolism in the liver. This is different from the rat where metabolic contribution of cytosolic CES to pyrethroid hydrolysis in plasma is also active. As CESs are not present in human plasma, no significant hydrolysis of pyrethroids in plasma is expected in humans (Crow *et al.*, 2007).

Model Parameters

Physiological Parameters

Age-specific human physiological parameters, including body weight (BW), cardiac output, tissue weights (or volumes), and tissue plasma flows, were adapted from published life-stage models (Clewell *et al.*, 2004; Ruark *et al.*, 2017; Song *et al.*, 2016; Wu *et al.*, 2015). These published life-stage models use the age-specific physiological parameters of women, which were adapted to represent men based on the most recent National Health and Nutrition Examination Survey (2005–2006) data. Growth curves for men and women used for modeling in this article are summarized in the Supplementary 1.

Chemical-Specific Parameters

All other parameters are taken from the rat model (Song *et al.*, 2019) and are listed in Supplementary 2, Table 1S. Assuming similarities in tissue composition between rat and human, the rat tissue partition coefficients were adapted for the human model. Tissue permeability-area cross products for diffusion were scaled to tissue volume^{0.75} instead of using a fixed value for all ages to reflect the diffusion surface area changes during growth. The values were adapted from the rat model.

Enzyme Ontogeny

It is critical to obtain enzyme ontogeny data to apply *in vitro* metabolism data collected using expressed enzymes to predict age-specific metabolic clearance of pyrethroids *in vivo* (Hines, 2013; Yoon and Clewell, 2016). We collected the enzyme ontogeny information for the CYP and CES enzymes contributing to metabolism of 8 pyrethroids: (1) DLM, (2) CPM, (3) TPM, (4) esfenvalerate, (5) bifenthrin, (6) cyphenothrin, (7) cyhalothrin, and (8) cyfluthrin and conducted nonlinear regression analyses of those age-specific protein expression data from birth to young adulthood reported in the literature (Hines, 2008; Hines *et al.*, 2016; McCarver *et al.*, 2014; Song *et al.*, 2016). Lognormal, hyperbolic, allosteric-sigmoidal, dose-response and, Gompertz growth curves were used, among which the best fit curve based on the Akaike Information Criterion and visual inspection was chosen to describe the maturation profiles of each enzyme expression as a fraction of the adult expression. Data are provided in Supplementary 3. In general, the data were best described as fractional expression of adult by hyperbolic, sigmoidal, or Gompertz models as follows:

$$(1) \text{ Hyperbolic eqn : } \frac{\text{Adultmax} \times \text{Age}}{\text{A50\%} + \text{Age}},$$

$$(2) \text{ Sigmoidal eqn : } \frac{\text{Adultmax} \times \text{Age}^h}{\text{Age}^{50\%h} + \text{Age}^h},$$

$$(3) \text{ Gompertz eqn : } \text{Adultmax} \times \frac{e^{\ln(\text{Adultmin}/\text{Adultmax})}}{e^{(-\text{Adult}50\% \times \text{Age})}},$$

where Adultmax is the maximum fractional expression of enzyme, Adultmin is the minimum fractional expression of enzyme (Y-intercept), A50% indicates age at which half-maximal fractional expression of enzyme is observed, Age is the actual age of the child, and h is the hill slope that reflects the steepness of the curve and presence of cooperativity. Gompertz model describes the ontogeny of most enzymes, including CYPs (1A2, 2C9, 2C19, 3A4) and CES, whereas the hyperbolic model ($n=1$) was adequate for CYP2B6, and sigmoidal model fitted better for CYP2C8.

In Vitro to In Vivo Extrapolation

The total intrinsic clearance of a given pyrethroid *in vivo* ($CL_{\text{int, vivo, total}}$) was calculated as the sum of enzyme-specific *in vivo* intrinsic clearance ($CL_{\text{int, vivo}}$) for all the enzymes that contribute to the metabolism of the pyrethroid. The enzyme-specific CL_{int} for each enzyme *in vivo* was extrapolated from the corresponding *in vitro* CL_{int} ($CL_{\text{int, vitro}}$) determined using the expressed human CYP and CES enzymes systems (Hedges *et al.*, 2019a).

Determination of *in vitro* intrinsic clearance ($CL_{\text{int, vitro}}$). The total intrinsic clearance of 8 pyrethroids (DLM, CPM, TPM, esfenvalerate, bifenthrin, cyphenothrin, cyhalothrin, and cyfluthrin) was assessed in human liver microsomes (HLMs) and cytosol (Supplementary 3). Interindividual variability in human liver metabolism being well known, we chose to use pooled microsomes and cytosol (150 adults: 75 males and 75 females) to better represent average human values for the selected pyrethroids used in this study. Some preliminary studies (data not shown) showed that the metabolism of DLM in rat (as CL_{int}) determined

in hepatocytes was comparable to the estimates based on the sum of the results from microsomes and cytosol. Furthermore, we used liver microsomes and cytosol because these subcellular fractions had all the phase I enzymes responsible for pyrethroid metabolism (ie, CYP and CES enzymes). In the phase I studies, K_M and V_{max} (Michaelis-Menten method) were determined to estimate the apparent CL_{int} for pyrethroids DLM, CPM, and TPM (substrate concentration range 0.1–5 μM) with primary aim to develop the PBPK model based on the DLM model as generic model (experiment design can be found in [Hedges et al. \[2019a\]](#)). For the phase II studies (5 additional pyrethroids including bifenthrin), a faster and simpler method of estimating the apparent CL_{int} was determined for human prediction (data not published yet). The similar physiochemical properties for all pyrethroids indicate similar solubility and based on the K_M of DLM, CPM, and TPM, a substrate concentration below K_M (0.1 μM) was selected for CL_{int} to ensure linear velocity and proper estimation of CL_{int} . For the expressed enzymes, K_M and V_{max} were not determined, apparent CL_{int} were obtained from metabolism of 0.1 μM pyrethroid (experiment design can be found in [Hedges et al. \[2019b\]](#)). To determine individual enzyme's contribution toward this total intrinsic clearance, enzyme-specific CL_{int_vitro} for each CYP and CES enzymes were adjusted by enzyme abundance for a specific age. Among the CYP and CES enzymes screened, only the enzymes showing activity toward the 8 pyrethroids metabolism were used for IVIVE: CYP1A2, CYP2B6, CYP2C8, CYP2C9, CYP2C19, CYP2D6, CYP3A4, CYP3A5, CES1, and CES2 ([Hedges et al., 2019b](#)). Details on the experiment design and results in both systems can be found in [Hedges et al. \(2019a,b\)](#).

Scaling process. The CL_{int_vitro} from each expressed human enzyme was scaled to the corresponding *in vivo* CL_{int} in order to obtain the total CL_{int_vivo} for metabolism of a given pyrethroid in human liver. Inter-System Extrapolation Factors (ISEFs) were used for conducting IVIVE of the expressed enzyme CL_{int_vitro} values along with the (1) microsomal or cytosolic protein content, (2) liver weight, and (3) enzyme abundance in the target age populations ([Yoon and Clewell, 2016](#); [Yoon et al., 2012](#)). ISEF values used in this study are from [Wetmore et al. \(2014\)](#) and the age-dependent Microsomal protein per gram of liver (MPPGL) values are from [Barter et al. \(2008\)](#). Cytosolic protein per gram liver (CPPGL) was used to perform IVIVE of cytosolic CES1 and 2, whereas MPPGL was used for CYPs and microsomal CESs. Contrary to MPPGL, there is little data available for age-dependent changes in CPPGL in the literature. For the adult, 80.7 mg CPPGL is reported ([Houston and Galetin, 2008](#)). Assuming that the ratio of MPPGL/ CPPGL would be constant across ages, age-specific CPPGL values were calculated. Equations used for modeling MPPGL and CPPGL in this study are summarized in [Supplementary 3](#). Information on the abundance of each CYP enzyme in adult liver for this calculation was taken from the published meta-analysis of several population studies ([Achour et al., 2014](#)). For CES enzymes, published data were used ([Boberg et al., 2017](#)). In [Boberg et al. \(2017\)](#), the abundance of each CES was given, except for cytosolic CES2 (CES2c). CES2c abundance was calculated based on the relative abundance of this enzyme, compared with the microsomal CES2 (CES2m) using the expression level ratio of CES2m/CES2c from [Hines et al. \(2016\)](#). The total intrinsic clearance for all CES enzymes *in vivo* in adults was calculated as the sum of microsomal and cytosolic CES enzymes' CL_{int_vivo} values obtained using [equations 2 and 3](#), respectively.

The relative contribution of the individual enzyme (CYPs and CESs) to the total *in vivo* CL_{int_vivo} (expressed as %) of a given

pyrethroid is calculated as described below ([equation 4](#)). For each individual enzyme, the ontogeny was expressed as fractions of adult expression over time. To obtain an age-specific intrinsic clearance *in vivo* for each enzyme, the adult intrinsic clearance for the corresponding enzyme ($CL_{int_enzyme_vivo_adult}$) was scaled based on the enzyme ontogeny. The estimated CL_{int_vivo} values for each enzyme at a given age were then summed to calculate the total liver intrinsic metabolic clearance ($CL_{int_vivo_total}$) of a given pyrethroid for that age *in vivo*. All the final *in vivo* clearance values for all the ages are provided in [Supplementary 3](#): final clearance values.

$$CL_{int_CYP_vivo_adult} = CL_{int_CYP_vitro} \times ISEF_CYP \times MPPGL \times LW \times CYP_abundance, \quad (1)$$

$$CL_{int_CESm_vivo_adult} = CL_{int_CESm_vitro} \times ISEF_CES \times MPPGL \times LW \times CESm_abundance, \quad (2)$$

$$CL_{int_CESc_vivo_adult} = CL_{int_CESc_vitro} \times ISEF_CES \times CPPGL \times LW \times CESc_abundance, \quad (3)$$

$$\% \text{ Contribution} = \frac{CL_{int_enzyme_vivo_adult}}{\text{Total hepatic } CL_{int_vivo_adult}} \times 100. \quad (4)$$

In the PBPK model, the total CL_{int_vivo} of a pyrethroid estimated from *in vitro* data ([equation 5](#)) is referred to as $CL_{int_vivo_estimated}$. As noted previously, an empirical free concentration adjustment factor (KMF) was applied to adjust this *in vivo* hepatic CL_{int} ($CL_{int_vivo_estimated}$) to obtain the actual CL_{int_vivo} :

$$CL_{int_vivo} = \frac{CL_{int_vivo_estimated}}{KMF}. \quad (5)$$

A single value of KMF was used for all 8 pyrethroids and for all the ages simulated in this study as this factor was shown to be applicable in describing the observed restricted clearance *in vivo* regardless of pyrethroid identity or age of the animals in the rat study ([Song et al., 2019](#)).

Sensitivity Analysis and Uncertainty

To evaluate the relative impact of each of the model parameters on the selected measure of internal exposure, in this study the maximum concentration (C_{max}) in the brain, a sensitivity analysis (SA) was performed. In our preliminary simulations, SA was not affected by a low or high dose (data not shown), hence in the current study, the SA was conducted for two ages (1 and 25 years old) and at one dose (1 mg/kg BW). The SA was also conducted at steady state (last C_{max} at steady state corresponding to 119–120 days). The sensitivity coefficient (SC) for each parameter analyzed was calculated as below ([Yoon et al., 2009](#)):

$$SC = \frac{\text{fractional change in model output/}}{\text{fractional change in parameter.}} \quad (6)$$

After oral exposure, each parameter was individually increased by 1% of their original value, whereas the other parameters were held constant to determine the SC values. All the parameters from [Supplementary Table 1S](#) in [Supplementary 2](#) were changed during the SA with the exception of the body surface area, the fraction of blood in tissue, and the air blood partition coefficient. A SC of 1 represents 1:1 relationship between the change in the parameter and the internal dose metric of choice. A negative SC indicates the given parameter influences

the dose metric in an inverse (opposite) direction. The SCs are grouped in 3 categories, high (absolute values ≥ 0.5), medium (absolute values ≥ 0.2 but < 0.5), or low (absolute values ≥ 0.1 but < 0.2), according to the International Program on Chemical Safety guideline (World Health Organization, 2010).

Model Simulations

The model was developed in acslX (version 3.1.4.2; The Aegis Technologies Group, Inc, Huntsville, Alabama) and was translated to R (model equations available in Supplementary 4). The R model was run using the model interface, PLETHEM (Pendse et al., submitted), for all model simulations.

Some simulations of the kinetic profile of the 8 pyrethroids in brain after a single oral dose every day during 14 days in adult (25Y) and children (1Y) can be found in Supplementary 2, Figure S5. Steady state is reached at 120 days but in the purpose of showing the kinetic profile, we stopped the simulation at 14 days.

The model for the 8 pyrethroids was run with a daily oral dose of 1 mg/kg with Monte-Carlo (MC) analysis in males of four different ages (1-, 5-, 19-, and 25-year old) to compare the internal exposure in the target tissue brain (C_{max}) across ages. Environmental Protection Agency has identified young children as a population of concern because dietary assessment identified this age group as the most highly exposed as children are still engaged in hand-to-mouth activities and have significant contact with treated surfaces (eg, carpet, turf, and pets).

Monte-Carlo simulations were performed with 1000 iterations to perform population-level simulations, at which the convergence was achieved. Further increase in the number of iterations to 5000 and 10 000 did not make a substantial difference in the convergence achievement. Monte-Carlo analysis was performed to incorporate interindividual variation in the values of parameters across the population to predict the distribution of internal doses. Based on the SA, parameters with SC over 0.2 were varied for MC analysis and were randomly sampled from their distributions, whereas other parameters were fixed. Model parameters that varied for the MC analysis and their distributions are listed in Table 1.

Price et al. (2003) showed that for the physiological parameters used in our MC analysis, the coefficient of variation (CV) between children and adult do not vary substantially (Price et al., 2003). To avoid the selection of extreme outliers, distributions were symmetrically truncated. For the parameters with a normal distribution in MC, we applied a truncation above and below two standard deviations (SD) from the mean. Parameters with a lognormal distribution are defined using the mean and SD of the log-transformed distribution. The truncation was applied to the transformed distribution in the same way as to the normal distribution.

RESULTS

Development of Enzyme Ontogeny

In vitro expressed enzyme studies indicated that CYP1A2, CYP3A4, CYP2C9, CYP2C19, CYP2B6, CYP2C8, CYP3A5, CES1-m, CES1-c, CES2-m, and CES2-c exhibit metabolic activity toward the 8 pyrethroids (data not shown). Maturation profiles vary for different enzymes (Figure 3 and Supplementary 3); for example, CES enzymes are expressed at adult levels at 6 months of age, whereas CYP1A2 and 2C19 are expressed at or near adult levels by 5–10 years old. For all the other enzymes analyzed in this study, their expression increases during the first 6 months of

Table 1. Parameters Changed for the Monte-Carlo Analysis

Parameters	Distribution ^a	CV	Reference
Body weight (BW)	L	0.22	Price et al. (2003)
Hematocrit (HTC)	L	0.06	Price et al. (2003)
Cardiac output (CARDOUTPC)	L	0.2	Thomas et al. (1996)
Fraction unbound in plasma (FuPLS)	L	0.1	Sethi et al. (2016)
Brain fractional plasma flow (FRBRNC)	N	0.1	Price et al. (2003)
Brain partition coef- ficient (PBRN)	L	0.3	Clewell et al. (1999)
Brain permeability (PABC)	L	0.3	Assumption
Liver volume (VOLLIVERC)	N	0.16	Price et al. (2003)
Liver fractional plasma flow (FRLIVC)	N	0.16	Price et al. (2003)
Metabolic constant (VKM1C)	L	0.5	Thomas et al. (1996)
Empirical adjust- ment factor (KMF)	L	0.5	Assumption
Fat volume (VOLFATC)	N	0.41	Price et al. (2003)
Fraction absorbed to systemic circula- tion (SWH)	L	1.44	Calculated based on O'Driscoll (2002)

^aSample distributions obtained from Portier and Kaplan (1989) (N, normal; L, log-normal) (Portier and Kaplan, 1989).

life to a level that is close to that of the adult (approximately 80%) and reach the adult level just thereafter.

Metabolism Profiles

Metabolism profiles and rates are similar for DLM, TPM, and cyphenothrin, likewise, CPM has comparable profiles to esfenvalerate, cyhalothrin, and cyfluthrin, whereas bifenthrin is quite distinct from others in its metabolism profile (Figure 4 and Supplementary 2, Figure 1S). Therefore, 3 pyrethroids were selected as representatives of all 8 pyrethroids in this article, the 5 remaining pyrethroids results are included in the Supplementary Files. These 3 pyrethroids are DLM (metabolized mainly by CES enzymes), CPM (metabolized by CYP and CES enzymes), and bifenthrin (metabolized only by CYP enzymes). The relative contribution of individual enzyme to the overall CL_{int} of DLM, CPM, and bifenthrin at different ages is shown in Figure 4. For DLM, enzyme contribution followed the order: CES1-m > CES1-c > CYP3A4 > CYP2C19 > CYP2B6 > CYP1A2 > CES2-m \approx CES2-c. For CPM, enzyme contribution followed the order: CES1-m > CES1-c > CES2-c > CES2-m > CYP2C19 > CYP2B6 > CYP2C9 > CYP3A4. For bifenthrin, enzyme contribution followed the order: CYP2C19 > CYP2C9 > CYP3A4 > CYP2C8 > CYP3A5. CYP3A5 and 2D6 have not been incorporated into the analysis, due to their negligible contribution of < 0.5%. Figure 4 clearly shows how different the enzyme contribution profiles are for these 3 representative pyrethroids, indicating that CESs are the major players in the metabolism of DLM and CPM with more than 70% contribution, whereas CYPs are mostly implicated in the metabolism of other pyrethroids, in particular, bifenthrin. The relative contribution of each enzyme for all

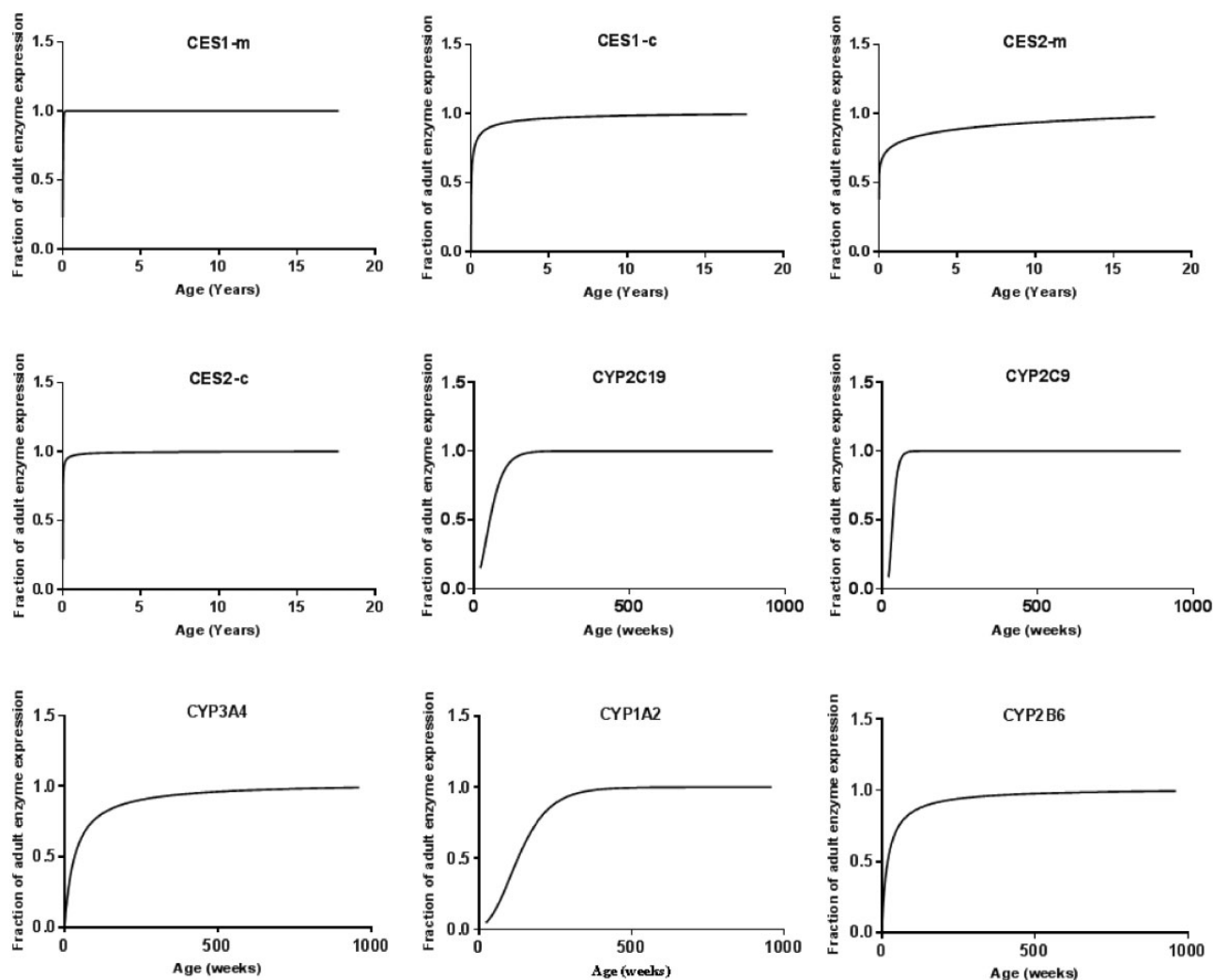


Figure 3. Nonlinear regression fits for major hepatic xenobiotic metabolizing enzymes involved in pyrethroid metabolism. Here, “m” represents the carboxylesterase (CES) enzyme in microsomes and “c” represents that in cytosol.

other pyrethroids to total metabolism at different ages is provided in [Supplementary 2, Figure 1S](#), and [Supplementary 3](#).

Estimation of the Age-Specific Intrinsic Clearance for a Pyrethroid *In Vivo*

The *in vivo* CL_{int} values that were calculated from IVIVE for DLM, CPM, and bifenthrin using the expressed enzyme data and the total CL_{int_vivo} from cytosol and microsomes are shown in [Figure 5](#). CL_{int_vivo} values for the 5 other pyrethroids are provided in [Supplementary 2, Figure S2](#). The expressed enzyme results were used to calculate relative contribution of each enzyme to the total CL_{int_vivo} of a given pyrethroid, whereas the pooled microsomal and cytosolic CL_{int_vivo} data for the pyrethroid were used to estimate the total CL_{int_vivo} . When adjusted to age-specific BW, for all 3 representative pyrethroids (DLM, CPM, and bifenthrin), there is no differences in the CL_{int} *in vivo* between ages.

Sensitivity analysis. Most of our model parameters are reported to have medium or low uncertainty. [Figure 6](#) presents SA results for brain concentration (C_{max}) for DLM, CPM, and bifenthrin that hold similar ranking among all 8 pyrethroids. Sensitivity

analysis results for the 5 other pyrethroids are provided in [Supplementary 2, Figure S3](#). Overall, our SA shows that brain partition coefficient and unbound fraction in plasma are the most sensitive parameters for all 8 pyrethroids.

Other physiological parameters that were highly sensitive for most of the 8 pyrethroids, includes BW, cardiac output, hematocrit, plasma flow to the liver, and fat volume. For early ages, the plasma flow to the brain, the liver, and fat volume and the rapidly perfused tissues were sensitive parameters. Hematocrit (HCT) was more sensitive for DLM compared with CPM. Hematocrit refers to the percentage of total blood volume composed of RBCs and thus determines the plasma volume in our model as described in $V_{plasma} = V_{blood} \times (1 - HCT)$. Pyrethroids are bound to plasma proteins and only the unbound fractions are subjected to clearance. With higher value of HCT, the plasma volume will be lower which will reflect as less protein binding and higher free fraction (Fu_{PLS}) available for clearance. Clearance of DLM is higher than CPM with similar protein binding. Thus, the amount of compound in the plasma available for clearance will be more important for DLM than CPM. Hence in sensitive analysis, when HCT is varied its influence is weightier for DLM than CPM.

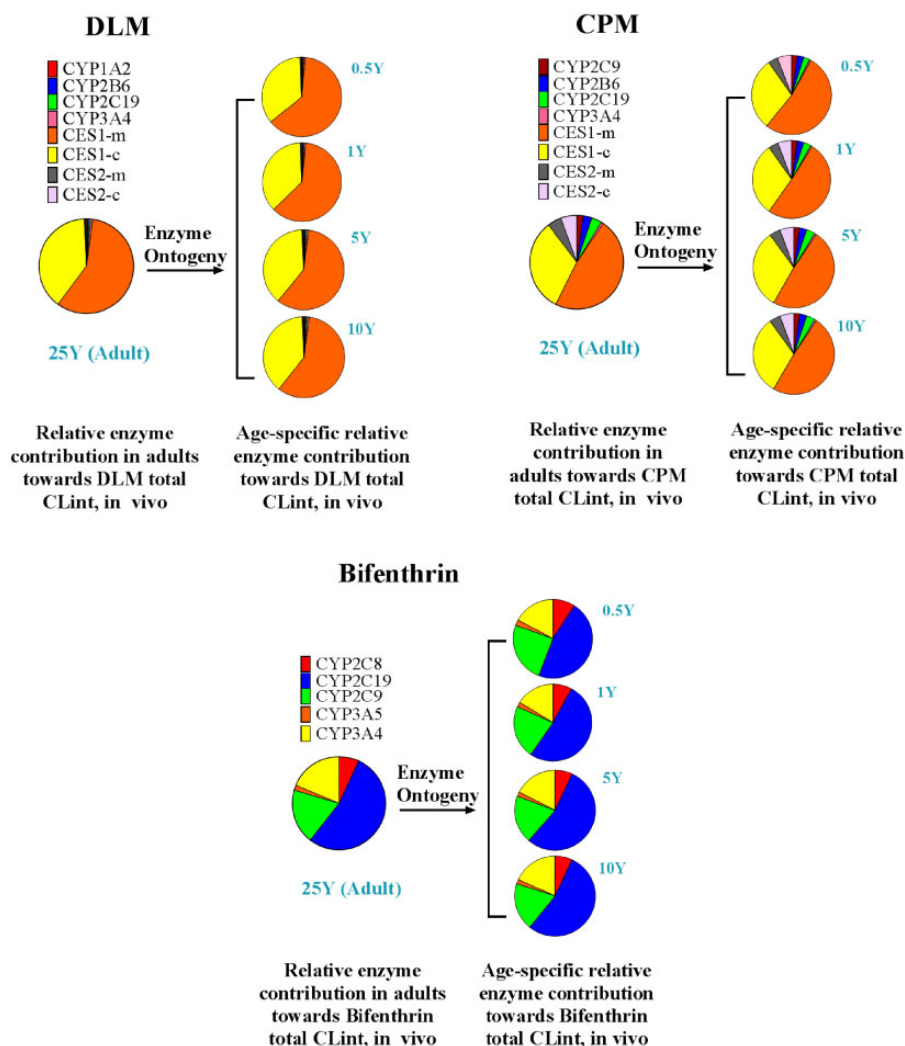


Figure 4. Relative contribution of cytochrome P450 (CYP) and CES enzymes to the metabolism of deltamethrin (DLM), cis-permethrin (CPM), and bifenthrin. Microsomal CES1 is denoted by CES1-m, cytosolic CES1 by CES1-c, microsomal CES2 by CES2-m, and cytosolic CES2 by CES2-c.

Liver metabolic clearance was a highly sensitive parameter for CPM and bifenthrin, however, it showed low to moderate sensitivity for DLM at early ages and adult, respectively. DLM, CPM, and bifenthrin are all rapidly cleared by metabolism in early and adult ages, but DLM metabolism is faster than that of CPM and bifenthrin (due to DLM being metabolized mainly by CES) making a difference in the sensitivity of metabolic clearance to brain C_{max} among the 3 compounds. For CPM and bifenthrin, the most sensitive parameters also included the brain partition coefficient, followed, in order, by $K_{MF} >$ the liver metabolic clearance $>$ the liver volume $>$ the unbound fraction in plasma $>$ the lymphatic absorption. Brain permeability is less sensitive for all the pyrethroids.

The LYMPSWTCH parameter is more sensitive for DLM compared with CPM. The LYMPSWTCH parameter corrects for the differing contribution of lymphatic absorption after oral exposure as fraction of total absorption. It is known that absorption of a highly lipophilic compound or drug with $\log P > 5$ occurs through lymphatic vessels to a varying extent depending on the fat content in diet in addition to the usual absorption path through portal veins (Charman and Stella, 1986; Jandacek et al., 2009). Deltamethrin is known to have a $\log K_{ow}$ of 4.61, whereas the $\log K_{ow}$ for CPM is 6.1. The difference in the chemical

structure may explain the difference in sensitivity for the lymphatic absorption.

The uncertainty of a model reflects the level of confidence in model predictions. A sensitivity/uncertainty matrix can be used to determine the overall importance of a parameter—our analysis was intended to be qualitative mainly to identify the areas for future studies/data collection. Two matrices for DLM and CPM are shown in Supplementary Table 2S in Supplementary 2. The parameters included in these 2 matrices are the ones that showed sensitivity in the SA. The lymphatic absorption as well as K_{MF} and the brain permeability show some uncertainty. Indeed, the lymphatic absorption parameter was calculated based on the literature and the K_{MF} parameter was introduced to the model to reduce the clearance to better fit the *in vivo* data. Permeability parameters were estimated which increase the uncertainty of the model, especially in brain, the target organ. This matrix was done for DLM and CPM only because they were the 2 pyrethroids originally used to develop the life-stage PBPK model. However, the uncertainty would remain the same for the 6 additional pyrethroids.

Simulation of pyrethroid internal exposure in different ages. The *in vivo* hepatic intrinsic clearances ($CL_{int, vivo}$) for DLM, CPM, and

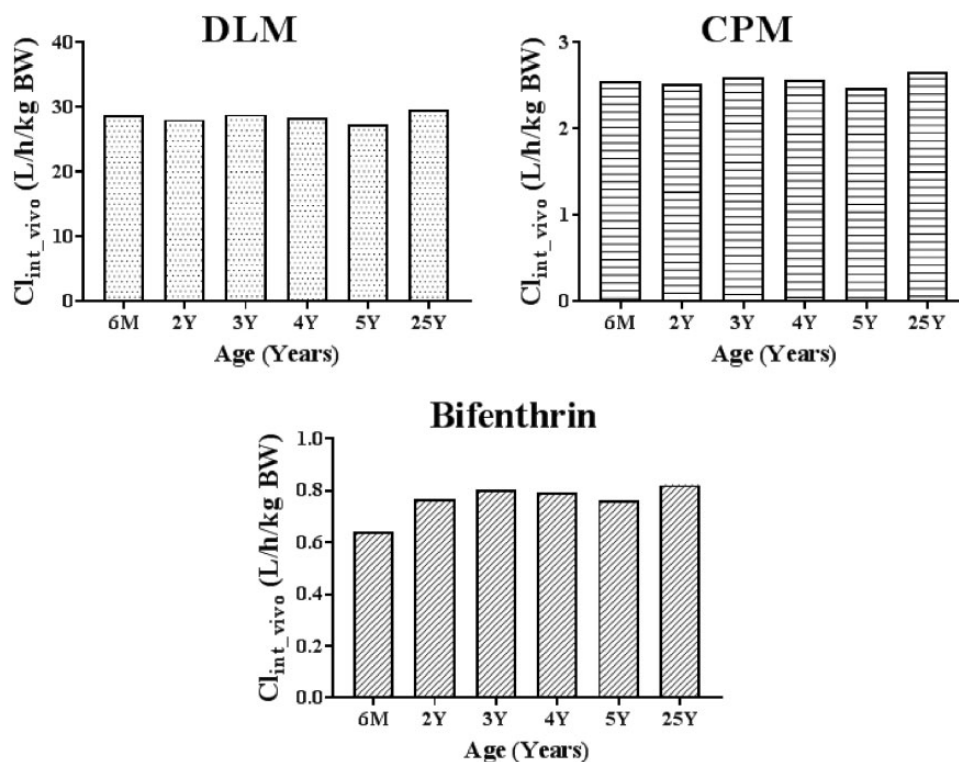


Figure 5. Intrinsic hepatic clearance of DLM, CPM, and bifenthrin in males of different ages.

bifenthrin are listed in Table 2. Hepatic metabolic clearance of a pyrethroid in our model is determined by 4 factors: hepatic CL_{int_vivo} , hepatic blood flow (QLIV), unbound fraction in plasma (FuPLS), and the free concentration adjustment factor, KMF. For DLM, CPM, and bifenthrin, the CL_{int_vivo} vary slightly with age. Only bifenthrin has a CL_{int_vivo} lower than the liver plasma flow at younger ages.

The mean C_{max} in brain following a daily single oral dose (1 mg/kg) of each pyrethroid for 120 days in males of 4 different ages was obtained by MC simulations. Our model simulation showed that the difference in internal exposure (C_{max}) at the target tissue (brain) in child (1Y, 5Y, 19Y) is similar to that in adults (25Y) for all 3 representative pyrethroids, DLM, CPM, and bifenthrin (Figure 7). The results for the 5 other pyrethroids are provided in Supplementary 2, Figure S4.

DISCUSSION

This research describes the development and application of an IVIVE supported life-stage human PBPK model for the evaluation of age-related sensitivity to pyrethroids exposure.

Studies indicate age-related differences in internal exposure to pyrethroids in the brain (Shafer et al., 2005; Sheets et al., 1994). Our rat model (Song et al., 2019) demonstrates that the observed age-related differences are largely determined by the differences in metabolic capacity for pyrethroids between the young and the adult and secondarily by age-related changes in physiology. To evaluate the human relevance of this, understanding and consideration of the ontogeny of pyrethroid metabolizing enzymes is critical. Several investigations have reported enzyme ontogeny for human hepatic xenobiotic metabolizing enzymes (Boberg et al., 2017; Hines et al., 2016; Pearce et al., 2016; Sadler et al., 2016; Yang et al., 2009; Zhu et al., 2009). However,

uncertainties still exist for many of these ontogeny data as the pediatric sample size and quality varied widely in these investigations. Another confounding factor is targeted age groups; for some studies, small sample size for early ages underrepresented their ontogeny trajectory, whereas for other studies, limited number of samples was distributed over the full pediatric age range. We therefore generated ontogeny profile for enzymes involved in pyrethroid metabolism as a continuous function using the protein expression data from collaborative efforts with Dr. Ron Hines (data not published) allowing development of equations to predict enzyme expression at any desired age from birth to adulthood.

The expressed enzyme-based IVIVE approach was employed to tackle the challenge of obtaining pediatric liver tissue samples, as well as uncertainties in the *in vitro* metabolic constants obtained from them. In fact, scaling *in vitro* measured metabolic constant to *in vivo* metabolism parameters has become common practice in pharmaceutical PBPK models for pediatrics (Barrett et al., 2012; Johnson et al., 2006; Maharaj et al., 2014). Using the expressed enzyme-based IVIVE, *in vivo* metabolic clearance was higher than that from subcellular fraction-based IVIVE for most of the tested pyrethroids. For example, total *in vivo* CL_{int} values estimated with expressed enzymes for DLM and CPM were 36,782 and 70,481/h/kg liver, respectively, but with HLMs and cytosol (subcellular fraction), the total CL_{int_vivo} were estimated to be 7,418 and 6,681/h/kg liver, respectively (data not shown). Whereas for bifenthrin, the CL_{int_vivo} values were similar in the two systems (145 and 2,061/h/kg liver for expressed enzymes and subcellular fraction, respectively). Variability in enzyme abundance in humans potentially explains the differences in the estimated *in vivo* clearance values between the two systems. For the current IVIVE approach, protein levels of CES1 and CES2 reported in Boberg et al. (2017) were used (most recent report based on a large cohort of well-

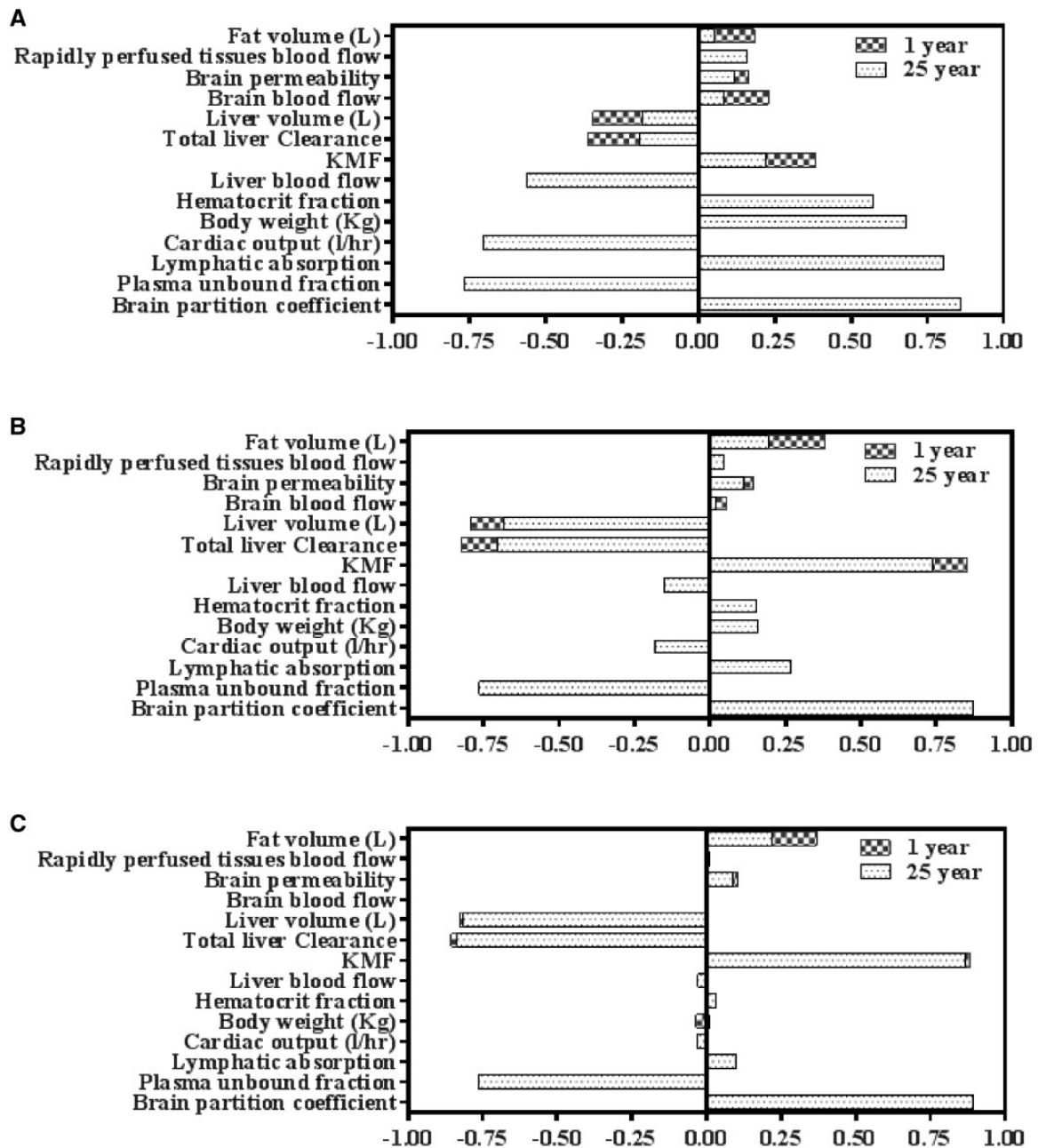


Figure 6. Sensitivity analysis indices after oral absorption for DLM (A), CPM (B), and bifenthrin (C). C_{max} in brain was evaluated during the sensitivity analysis.

Table 2. Model Estimated Hepatic Intrinsic Clearance ($CL_{int,vivo}$) for DLM, CPM, and Bifenthrin in the Male

Age (year)	QLIV (l/h)	DLM Hepatic $CL_{int,vivo}$ (l/h)		CPM Hepatic $CL_{int,vivo}$ (l/h)		Bifenthrin Hepatic $CL_{int,vivo}$ (l/h)	
	Male	Male	Male	Male	Male	Male	Male
0.5	12.2	224		20		5	
2	18.3	375		34		10	
5	24.0	565		51		16	
12	38.3	1282		115		36	
19	49.9	2066		186		58	
25	50.7	2417		217		67	

characterized pediatric and adult subjects), which were higher than those reported in some other studies (Godin et al., 2006; Hedges et al., 2019a,b; McCarver et al., 2014; Sato et al., 2012).

Such differences in enzyme abundance in different reports might be due to the origin of microsomal samples or the accuracy of difference in the quantification methods used. However,

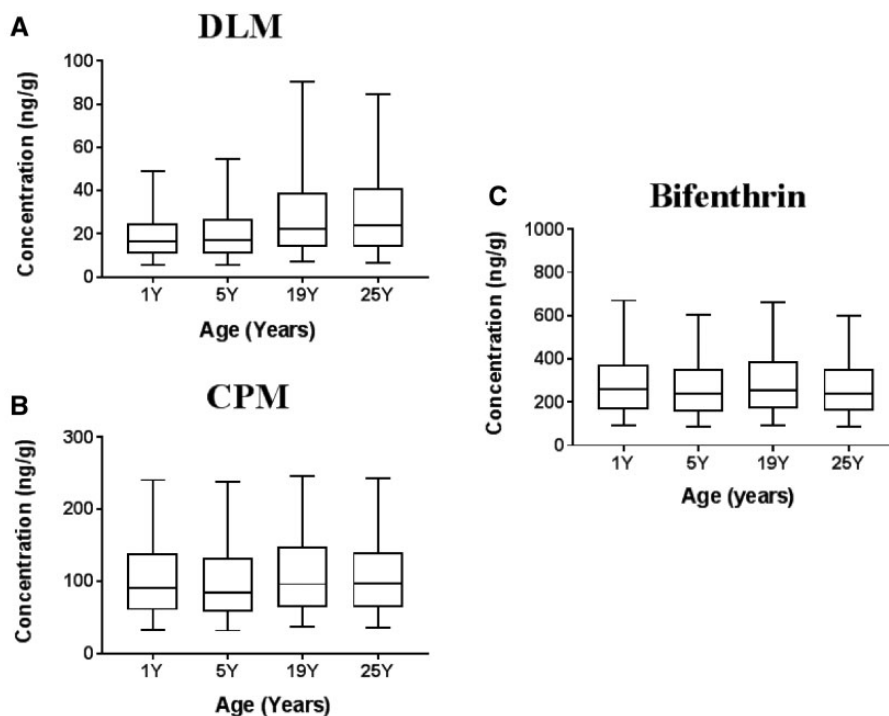


Figure 7. Brain C_{max} after a daily single DLM (A), CPM (B), and bifenthrin (C) oral dose at 1 mg/kg, respectively in males 4 different ages. One thousand individuals for each group were simulated. Horizontal line bisecting large rectangle, median; large rectangle, lower and upper quartiles; whiskers, 5th and 95th percentiles.

the differences in the estimates between the two systems are much less than the expected human variability inferred from the variation in metabolic enzyme abundances (Achour et al., 2014; Boberg et al., 2017; Kenyon et al., 2019). Therefore, the expressed enzyme results were used to calculate relative contribution of each enzyme to the total $CL_{int,vivo}$ of a given pyrethroid, whereas the pooled microsomal and cytosolic $CL_{int,vivo}$ data for the pyrethroid were used to estimate the total $CL_{int,vivo}$. These experiments were done in subcellular fraction and it is interesting to also look at the values in other systems like hepatocytes. In Willemin et al. (2015), they measured an *in vivo* CL_{int} for CPM in cryopreserved hepatocytes of 60 l/h/kg liver. Use of freshly isolated or cryopreserved primary hepatocytes in suspension for *in vitro* predictions for rapidly cleared chemicals is a more adequate system compared with other matrices. Although use of monolayer or sandwich-culture of hepatocytes extends viability but there is clear phenotypic instability and rapid decline of metabolic competence within a few hours (Di et al., 2012; Di and Obach, 2015). Further more, in Willemin study, the CYP activities of their hepatocyte lots were in the low range of activities reported by others. Hence, the differences in rate of metabolism are mostly due to differences in CYP content in the two different systems. Our *in vitro* metabolism data and IVIVE analysis showed that CES enzymes are the major contributor to metabolism in humans for most of the pyrethroids except for bifenthrin, for which CYPs were largely responsible for metabolism. For all of the 8 pyrethroids, the metabolism is very rapid, therefore the hepatic metabolism is only limited by liver blood flow regardless of age in humans. This holds true for bifenthrin as well but only for adults. In younger ages, metabolism is a limiting factor. The sum of CES1 levels in both liver microsomes and cytosol, is around 30 times that of microsomal CYP3A4 (Achour et al., 2014) resulting in a very efficient hydrolysis of the compound metabolized by this class of enzyme. In addition, total *in vivo* hepatic clearance of each pyrethroid in early

ages would be higher than that in adults, even if there is no difference in hepatic $CL_{int,vivo}$ (Figure 5), as the relative liver blood flow and liver weight are both higher per BW in early ages. Note that relative values are referred to here as the absolute liver weight or liver plasma flow increase with age, but their fraction of the total BW or total cardiac output, respectively, decreases. These age-dependent changes in physiological factors together with the rapid metabolic clearance contribute to an internal exposure in the target tissue in children lower than or comparable to that in adults in humans in response to the same level of exposure to a given pyrethroid.

Restrictive clearance was used to account for the difference between *in vitro*-derived and *in vivo*-derived intrinsic clearance observed, as was done in the rat (Song et al., 2019). Other pyrethroid PBPK models (Godin et al., 2010; Mirfazaelian et al., 2006; Tornero-Velez et al., 2010) fit the plasma time course data reasonably well without adjusting *in vitro* clearance rates and do not separate the free and bound fractions of pyrethroids (Tornero-Velez et al., 2012). It is now known that nonspecific, noncovalent binding of pyrethroids to microsomes was likely in the *in vitro* incubation conditions used to parameterize these models. As a result, the nonspecific binding *in vitro* would mask the restricted clearance of pyrethroids *in vivo*. Importantly, it should be noted that the current description of restricted clearance in the PBPK model does not imply that clearance of pyrethroids is slow. Although clearance is reduced, pyrethroids are rapidly and completely cleared from the body at doses relevant to actual human exposure as indicated by results from human volunteer studies using several pyrethroids (Ratelle et al., 2015a,b).

Another factor in the predicted clearance is the fraction of lymphatic absorption. Higher lymphatic absorption was used in the rat than in the human model. Lymphatic absorption is well known for highly lipophilic drugs and chemicals, the degree of which varies in humans ranging from 1% to 45% depending on

coadministration of lipid-based formulations or in the presence of food (O'Driscoll, 2002). Considering the expected substantial degree of human variability in intestinal lipid content, the degree of lymphatic absorption is likely highly variable.

Some juvenile animal studies have raised concerns for potentially higher sensitivities to the effect of pyrethroid exposure in infants and children (Sheets et al., 1994). Our rat model data corroborates this pharmacokinetic determination of the sensitivity between young and adult rats (Song et al., 2019). In contrast, the human model represented in this manuscript did not predict any substantial difference in brain C_{max} in different age groups for any of the three case pyrethroids (Figure 7). Hepatic CYPs and CES are important metabolizing enzymes for detoxification and elimination of pyrethroids in both rats and humans (Anand et al., 2006; Crow et al., 2007; Godin et al., 2006, 2007; Scollon et al., 2009), but significant species differences exist in the relative contribution of various CYPs and CES enzymes (Godin et al., 2007; Scollon et al., 2009) as was confirmed by our *in vitro* expressed enzyme results. This species difference is likely one of the factors for the age-related sensitivity observed in rats but not in humans as the major enzyme for pyrethroid metabolism in human is CES, which shows a rapid maturation after birth. In fact, differences in the developmental changes in the expression of CYP and CES enzymes are evident between rats versus humans (Anand et al., 2006; Hines, 2008, 2012; Hines et al., 2016; Kim et al., 2010; Koukouritaki et al., 2004; Song et al., 2017; Stevens et al., 2003). The earlier maturation of metabolic competency of hepatic CYP and CES enzymes in humans likely allows juvenile humans to detoxify pyrethroids to a much greater extent compared with rats (Crow et al., 2007; Hines, 2012; Hines et al., 2016; Song et al., 2017). Collectively, the ontogeny of the pyrethroid metabolizing enzymes is a key driver for the age-related sensitivity observed in rats saturating the enzyme capacity in juvenile animals after the high dose used in the toxicity study (Sheets et al., 1994).

The ultimate goal of the life-stage IVIVE-PBPK modeling framework presented here is to support risk assessments for potentially sensitive populations of early ages for pyrethroids as a chemical class. From this perspective, the most important contribution of our case studies is a demonstration of the development of a generic model structure for pyrethroids using a common set of parameters apart from compound-specific metabolism. The clearance-based read-across strategy to address age-related sensitivity using life-stage PBPK models and IVIVE can be readily applied to other groups of chemicals and support internal exposure-based risk assessment for potentially sensitive populations.

SUPPLEMENTARY DATA

Supplementary data are available at *Toxicological Sciences* online.

DECLARATION OF CONFLICTING INTERESTS

The authors declared no potential conflicts of interest with respect to the research, authorship, and/or publication of this article.

ACKNOWLEDGMENTS

The authors thank Barbara Wetmore for her help in using the [Supplementary data](#) from her 2014 article. They acknowledge Mike Tornero-Velez for helpful discussion during

this project. The authors also thank the American Chemistry Council Long-range Research Initiative for supporting the core version of PLETHEM.

FUNDING

This work was supported by the Council for the Advancement of Pyrethroid Human Risk Assessment (CAPHRA), LLC.

REFERENCES

- Achour, B., Barber, J., and Rostami-Hodjegan, A. (2014). Expression of hepatic drug-metabolizing cytochrome p450 enzymes and their intercorrelations: A meta-analysis. *Drug Metab. Dispos.* **42**, 1349–1356.
- Anand, S. S., Kim, K. B., Padilla, S., Muralidhara, S., Kim, H. J., Fisher, J. W., and Bruckner, J. V. (2006). Ontogeny of hepatic and plasma metabolism of deltamethrin *in vitro*: Role in age-dependent acute neurotoxicity. *Drug Metab. Dispos.* **34**, 389–397.
- Barrett, J. S., Della Casa Alberighi, O., Läer, S., and Meibohm, B. (2012). Physiologically based pharmacokinetic (PBPK) modeling in children. *Clin. Pharmacol. Ther.* **92**, 40–49.
- Barter, Z. E., Chowdry, J. E., Harlow, J. R., Snawder, J. E., Lipscomb, J. C., and Rostami-Hodjegan, A. (2008). Covariation of human microsomal protein per gram of liver with age: Absence of influence of operator and sample storage may justify interlaboratory data pooling. *Drug Metab. Dispos.* **36**, 2405–2409.
- Boberg, M., Vrana, M., Mehrotra, A., Pearce, R. E., Gaedigk, A., Bhatt, D. K., Leeder, J. S., and Prasad, B. (2017). Age-dependent absolute abundance of hepatic carboxylesterases (CES1 and CES2) by LC-MS/MS proteomics: Application to PBPK modeling of oseltamivir *in vivo* pharmacokinetics in infants. *Drug Metab. Dispos.* **45**, 216–223.
- Charman, W. N. A., and Stella, V. J. (1986). Effects of lipid class and lipid vehicle volume on the intestinal lymphatic transport of DDT. *Int. J. Pharm.* **33**, 165–172.
- Clewell, H. J., 3rd, and Andersen, M. E. (1994). Physiologically-based pharmacokinetic modeling and bioactivation of xenobiotics. *Toxicol. Ind. Health* **10**, 1–24.
- Clewell, H. J., Gearhart, J. M., Gentry, P. R., Covington, T. R., VanLandingham, C. B., Crump, K. S., and Shipp, A. M. (1999). Evaluation of the uncertainty in an oral reference dose for methylmercury due to interindividual variability in pharmacokinetics. *Risk Anal.* **19**, 547–558.
- Clewell, H. J., Gentry, P. R., Covington, T. R., Sarangapani, R., and Teeguarden, J. G. (2004). Evaluation of the potential impact of age- and gender-specific pharmacokinetic differences on tissue dosimetry. *Toxicol. Sci.* **79**, 381–393.
- Crow, J. A., Borazjani, A., Potter, P. M., and Ross, M. K. (2007). Hydrolysis of pyrethroids by human and rat tissues: Examination of intestinal, liver and serum carboxylesterases. *Toxicol. Appl. Pharmacol.* **221**, 1–12.
- Di, L., Keefer, C., Scott, D. O., Strelevitz, T. J., Chang, G., Bi, Y. A., Lai, Y., Duckworth, J., Fenner, K., Troutman, M. D., et al. (2012). Mechanistic insights from comparing intrinsic clearance values between human liver microsomes and hepatocytes to guide drug design. *Eur. J. Med. Chem.* **57**, 441–448.
- Di, L., and Obach, R. S. (2015). Addressing the challenges of low clearance in drug research. *AAPS J.* **17**, 352–357.
- Godin, S. J., Crow, J. A., Scollon, E. J., Hughes, M. F., DeVito, M. J., and Ross, M. K. (2007). Identification of rat and human

- cytochrome p450 isoforms and a rat serum esterase that metabolize the pyrethroid insecticides deltamethrin and esfenvalerate. *Drug Metab. Dispos.* **35**, 1664–1671.
- Godin, S. J., DeVito, M. J., Hughes, M. F., Ross, D. G., Scollon, E. J., Starr, J. M., Setzer, R. W., Conolly, R. B., and Tornero-Velez, R. (2010). Physiologically based pharmacokinetic modeling of deltamethrin: development of a rat and human diffusion-limited model. *Toxicol. Sci.* **115**, 330–343.
- Godin, S. J., Scollon, E. J., Hughes, M. F., Potter, P. M., DeVito, M. J., and Ross, M. K. (2006). Species differences in the in vitro metabolism of deltamethrin and esfenvalerate: Differential oxidative and hydrolytic metabolism by humans and rats. *Drug Metab. Dispos.* **34**, 1764–1771.
- Hedges, L., Brown, S., MacLeod, A. K., Vardy, A., Doyle, E., Song, G., Moreau, M., Yoon, M., Osimitz, T. G., and Lake, B. G. (2019b). Metabolism of deltamethrin and cis- and trans-permethrin by human expressed cytochrome p450 and carboxylesterase enzymes. *Xenobiotica* **49**, 521–527.
- Hedges, L., Brown, S., Vardy, A., Doyle, E., Yoon, M., Osimitz, T. G., and Lake, B. G. (2019a). Metabolism of deltamethrin and cis- and trans-permethrin by rat and human liver microsomes, liver cytosol and plasma preparations. *Xenobiotica* **49**, 388–396.
- Hines, R. N. (2008). The ontogeny of drug metabolism enzymes and implications for adverse drug events. *Pharmacol. Ther.* **118**, 250–267.
- Hines, R. N. (2012). Age-dependent expression of human drug-metabolizing enzymes. *Encyclopedia of Drug Metabolism and Interactions*. (Lyubimov A. V., Ed), 1–24. John Wiley & Sons, Inc., Philadelphia.
- Hines, R. N. (2013). Developmental expression of drug metabolizing enzymes: Impact on disposition in neonates and young children. *Int. J. Pharm.* **452**, 3–7.
- Hines, R. N., Sargent, D., Autrup, H., Birnbaum, L. S., Brent, R. L., Doerr, N. G., Cohen Hubal, E. A., Juberg, D. R., Laurent, C., Luebke, R., et al. (2010). Approaches for assessing risks to sensitive populations: Lessons learned from evaluating risks in the pediatric population. *Toxicol. Sci.* **113**, 4–26.
- Hines, R. N., Simpson, P. M., and McCarver, D. G. (2016). Age-dependent human hepatic carboxylesterase 1 (CES1) and carboxylesterase 2 (CES2) postnatal ontogeny. *Drug Metab. Dispos.* **44**, 959–966.
- Houston, J. B., and Galetin, A. (2008). Methods for predicting in vivo pharmacokinetics using data from in vitro assays. *Curr. Drug Metab.* **9**, 940–951.
- Jandacek, R. J., Rider, T., Yang, Q., Woollett, L. A., and Tso, P. (2009). Lymphatic and portal vein absorption of organochlorine compounds in rats. *Am. J. Physiol. Gastrointest. Liver Physiol.* **296**, G226–G234.
- Johnson, T. N., Rostami-Hodjegan, A., and Tucker, G. T. (2006). Prediction of the clearance of eleven drugs and associated variability in neonates, infants and children. *Clin. Pharmacokinet.* **45**, 931–956.
- Kenyon, E. M., Lipscomb, J. C., Pegram, R. A., George, B. J., and Hines, R. N. (2019). The impact of scaling factor variability on risk-relevant pharmacokinetic outcomes in children: A case study using bromodichloromethane (BDCM). *Toxicol. Sci.* **167**, 347–359.
- Kim, K. B., Anand, S. S., Kim, H. J., White, C. A., and Bruckner, J. V. (2008). Toxicokinetics and tissue distribution of deltamethrin in adult Sprague-Dawley rats. *Toxicol. Sci.* **101**, 197–205.
- Kim, K. B., Anand, S. S., Kim, H. J., White, C. A., Fisher, J. W., Tornero-Velez, R., and Bruckner, J. V. (2010). Age, dose, and time-dependency of plasma and tissue distribution of deltamethrin in immature rats. *Toxicol. Sci.* **115**, 354–368.
- Koukouritaki, S. B., Manro, J. R., Marsh, S. A., Stevens, J. C., Rettie, A. E., McCarver, D. G., and Hines, R. N. (2004). Developmental expression of human hepatic cyp2c9 and cyp2c19. *J. Pharmacol. Exp. Ther.* **308**, 965–974.
- Maharaj, A. R., Barrett, J. S., and Edginton, A. N. (2014). Physiologically based pharmacokinetic modeling and simulation in pediatric drug development. *CPT Pharmacometrics Syst. Pharmacol.* **3**, e150.
- McCarver, D., He, J., Simpson, P., and Hines, R. N. (2014). Human hepatic CES1 and CES2 ontogeny. *Toxicologist* **138**, 48.
- Mirfazaelian, A., Kim, K. B., Anand, S. S., Kim, H. J., Tornero-Velez, R., Bruckner, J. V., and Fisher, J. W. (2006). Development of a physiologically based pharmacokinetic model for deltamethrin in the adult male Sprague-Dawley rat. *Toxicol. Sci.* **93**, 432–442.
- O'Driscoll, C. M. (2002). Lipid-based formulations for intestinal lymphatic delivery. *Eur. J. Pharm. Sci.* **15**, 405–415.
- Pearce, R. E., Gaedigk, R., Twist, G. P., Dai, H., Riffel, A. K., Leeder, J. S., and Gaedigk, A. (2016). Developmental expression of cyp2b6: A comprehensive analysis of mRNA expression, protein content and bupropion hydroxylase activity and the impact of genetic variation. *Drug Metab. Dispos.* **44**, 948–958.
- Pope, C. N., Karanth, S., Liu, J., and Yan, B. (2005). Comparative carboxylesterase activities in infant and adult liver and their in vitro sensitivity to chlorpyrifos oxon. *Regul. Toxicol. Pharmacol.* **42**, 64–69.
- Portier, C. J., and Kaplan, N. L. (1989). Variability of safe dose estimates when using complicated models of the carcinogenic process. A case study: Methylene chloride. *Fundam. Appl. Toxicol.* **13**, 533–544.
- Price, P. S., Conolly, R. B., Chaisson, C. F., Gross, E. A., Young, J. S., Mathis, E. T., and Tedder, D. R. (2003). Modeling interindividual variation in physiological factors used in PBPK models of humans. *Crit. Rev. Toxicol.* **33**, 469–503.
- Ratelle, M., Cote, J., and Bouchard, M. (2015a). Time profiles and toxicokinetic parameters of key biomarkers of exposure to cypermethrin in orally exposed volunteers compared with previously available kinetic data following permethrin exposure. *J. Appl. Toxicol.* **35**, 1586–1593.
- Ratelle, M., Cote, J., and Bouchard, M. (2015b). Toxicokinetics of permethrin biomarkers of exposure in orally exposed volunteers. *Toxicol. Lett.* **232**, 369–375.
- Ring, C. L., Pearce, R. G., Setzer, R. W., Wetmore, B. A., and Wambaugh, J. F. (2017). Identifying populations sensitive to environmental chemicals by simulating toxicokinetic variability. *Environ. Int.* **106**, 105–118.
- Ruark, C. D., Song, G., Yoon, M., Verner, M.-A., Andersen, M. E., Clewell, H. J., and Longnecker, M. P. (2017). Quantitative bias analysis for epidemiological associations of perfluoroalkyl substance serum concentrations and early onset of menopause. *Environ. Int.* **99**, 245–254.
- Sadler, N. C., Nandhikonda, P., Webb-Robertson, B. J., Ansong, C., Anderson, L. N., Smith, J. N., Corley, R. A., and Wright, A. T. (2016). Hepatic cytochrome p450 activity, abundance, and expression throughout human development. *Drug Metab. Dispos.* **44**, 984–991.
- Saghir, S. A., Khan, S. A., and McCoy, A. T. (2012). Ontogeny of mammalian metabolizing enzymes in humans and animals used in toxicological studies. *Crit. Rev. Toxicol.* **42**, 323–357.
- Sato, Y., Miyashita, A., Iwatsubo, T., and Usui, T. (2012). Simultaneous absolute protein quantification of carboxylesterases 1 and 2 in human liver tissue fractions using liquid chromatography-tandem mass spectrometry. *Drug Metab. Dispos.* **40**, 1389–1396.

- Scollon, E. J., Starr, J. M., Godin, S. J., DeVito, M. J., and Hughes, M. F. (2009). In vitro metabolism of pyrethroid pesticides by rat and human hepatic microsomes and cytochrome p450 isoforms. *Drug Metab. Dispos.* **37**, 221–228.
- Sethi, P. K., White, C. A., Cummings, B. S., Hines, R. N., Muralidhara, S., and Bruckner, J. V. (2016). Ontogeny of plasma proteins, albumin and binding of diazepam, cyclosporine, and deltamethrin. *Pediatr. Res.* **79**, 409–415.
- Shafer, T. J., Meyer, D. A., and Crofton, K. M. (2005). Developmental neurotoxicity of pyrethroid insecticides: Critical review and future research needs. *Environ. Health Perspect.* **113**, 123–136.
- Sheets, L. P., Doherty, J. D., Law, M. W., Reiter, L. W., and Crofton, K. M. (1994). Age-dependent differences in the susceptibility of rats to deltamethrin. *Toxicol. Appl. Pharmacol.* **126**, 186–190.
- Soderlund, D. M. (2012). Molecular mechanisms of pyrethroid insecticide neurotoxicity: Recent advances. *Arch. Toxicol.* **86**, 165–181.
- Song, G., Moreau, M., Efremenko, A., Lake, B. G., Wu, H., Bruckner, J. V., White, C. A., Osimitz, T. G., Creek, M. R., and Hinderliter, P. M., et al. (2019). Evaluation of age-related pyrethroid pharmacokinetic differences in rats: Physiologically-based pharmacokinetic model development using in vitro data and in vitro to in vivo extrapolation. *Toxicol. Sci.* **169**, 365–379.
- Song, G., Peeples, C. R., Yoon, M., Wu, H., Verner, M.-A., Andersen, M. E., Clewell, H. J., and Longnecker, M. P. (2016). Pharmacokinetic bias analysis of the epidemiological associations between serum polybrominated diphenyl ether (BDE-47) and timing of menarche. *Environ. Res.* **150**, 541–548.
- Song, G., Sun, X., Hines, R. N., McCarver, D. G., Lake, B. G., Osimitz, T. G., Creek, M. R., Clewell, H. J., and Yoon, M. (2017). Determination of human hepatic cyp2c8 and cyp1a2 age-dependent expression to support human health risk assessment for early ages. *Drug Metab. Dispos.* **45**, 468–475.
- Stevens, J. C., Hines, R. N., Gu, C., Koukouritaki, S. B., Manro, J. R., Tandler, P. J., and Zaya, M. J. (2003). Developmental expression of the major human hepatic cyp3a enzymes. *J. Pharmacol. Exp. Ther.* **307**, 573–582.
- Thomas, R. S., Lytle, W. E., Keefe, T. J., Constan, A. A., and Yang, R. S. (1996). Incorporating Monte Carlo simulation into physiologically based pharmacokinetic models using advanced continuous simulation language (ACSL): A computational method. *Fundam. Appl. Toxicol.* **31**, 19–28.
- Tornero-Velez, R., Davis, J., Scollon, E. J., Starr, J. M., Setzer, R. W., Goldsmith, M.-R., Chang, D. T., Xue, J., Zartarian, V., DeVito, M. J., et al. (2012). A pharmacokinetic model of cis- and trans-permethrin disposition in rats and humans with aggregate exposure application. *Toxicol. Sci.* **130**, 33–47.
- Tornero-Velez, R., Mirfazaelian, A., Kim, K. B., Anand, S. S., Kim, H. J., Haines, W. T., Bruckner, J. V., and Fisher, J. W. (2010). Evaluation of deltamethrin kinetics and dosimetry in the maturing rat using a PBPK model. *Toxicol. Appl. Pharmacol.* **244**, 208–217.
- Wetmore, B. A., Allen, B., Clewell, H. J., Parker, T., Wambaugh, J. F., Almond, L. M., Sochaski, M. A., and Thomas, R. S. (2014). Incorporating population variability and susceptible subpopulations into dosimetry for high-throughput toxicity testing. *Toxicol. Sci.* **142**, 210–224.
- World Health Organization (WHO). (2010). Characterization and Application of Physiologically Based Pharmacokinetic Models in Risk Assessment. World Health Organization, International Programme on Chemical Safety, Geneva, Switzerland.
- Willemin, M. E., Desmots, S., Le Grand, R., Lestremau, F., Zeman, F. A., Leclerc, E., Moesch, C., and Brochot, C. (2016). PBPK modeling of the cis- and trans-permethrin isomers and their major urinary metabolites in rats. *Toxicol. Appl. Pharmacol.* **294**, 65–77.
- Willemin, M. E., Kadar, A., de Sousa, G., Leclerc, E., Rahmani, R., and Brochot, C. (2015). In vitro human metabolism of permethrin isomers alone or as a mixture and the formation of the major metabolites in cryopreserved primary hepatocytes. *Toxicol. In Vitro* **29**, 803–812.
- Wu, H., Yoon, M., Verner, M.-A., Xue, J., Luo, M., Andersen, M. E., Longnecker, M. P., and Clewell, H. J. (2015). Can the observed association between serum perfluoroalkyl substances and delayed menarche be explained on the basis of puberty-related changes in physiology and pharmacokinetics? *Environ. Int.* **82**, 61–68.
- Yang, D., Pearce, R. E., Wang, X., Gaedigk, R., Wan, Y. J., and Yan, B. (2009). Human carboxylesterases HCE1 and HCE2: Ontogenic expression, inter-individual variability and differential hydrolysis of oseltamivir, aspirin, deltamethrin and permethrin. *Biochem. Pharmacol.* **77**, 238–247.
- Yoon, M., Campbell, J. L., Andersen, M. E., and Clewell, H. J. (2012). Quantitative in vitro to in vivo extrapolation of cell-based toxicity assay results. *Crit. Rev. Toxicol.* **42**, 633–652.
- Yoon, M., and Clewell, H. J. (2016). Addressing early life sensitivity using physiologically based pharmacokinetic modeling and in vitro to in vivo extrapolation. *Toxicol. Res.* **32**, 15–20.
- Yoon, M., Nong, A., Clewell, H. J., Taylor, M. D., Dorman, D. C., and Andersen, M. E. (2009). Lactational transfer of manganese in rats: Predicting manganese tissue concentration in the dam and pups from inhalation exposure with a pharmacokinetic model. *Toxicol. Sci.* **112**, 23–43.
- Zhu, H. J., Appel, D. I., Jiang, Y., and Markowitz, J. S. (2009). Age- and sex-related expression and activity of carboxylesterase 1 and 2 in mouse and human liver. *Drug Metab. Dispos.* **37**, 1819–1825.